Monograph:

eprints@whiterose.ac.uk
https://eprints.whiterose.ac.uk/

Identification of mill dynamics from normal operating records

by

S. A. Billings, R. G. Cheetham, M. Hamiane and A. S. Morris

Department of Control Engineering
University of Sheffield
Mappin Street
Sheffield   S1 3JD

1. Introduction

This report describes plant modelling based on data collected during routine operation at a large coal-fired power station in the north of England. Data from one of the eight pulverised fuel mills which feed the furnace of one of the generating units was recorded continuously on magnetic tape, and sampled using a digital computer at the University. Structural and parametric estimation was then performed using the multivariable system identification package (LMI) recently developed (Hamiane, 1984).

A brief description of mill operation is presented in Section 2, together with diagrams showing the principal inputs and outputs, and the basic processes operating within the mill. Section 3 describes data collection and preliminary correlation analysis. Structure detection and parameter estimation is conducted in Section 4 and the most appropriate multiple-input, single-output linear model is fitted. Model validity checks based on the prediction error are also demonstrated with conclusions presented in Section 5,

2. Pulverised Fuel Mill Operation

Pulverised fuel mill operation is illustrated in figure 2.1. Coal enters the mill via a conveyor belt, at a rate controlled by an operator or computer-set scoop position. The mill is rotated, grinding the coal by impact with steel balls. High velocity air supplied by the primary air (PA) fan carries the grinding product into the body of the mill where classification takes place in two basic steps. Particles whose free-fall velocity is greater than the local upward air velocity fall and recombine with the feed. Following coarse classification lighter particles are carried to the fine classifier where further particles are rejected and recirculate. Secondary classification is by cyclone action; air rotating at a controlled rate causes particles heavier than the requisite size to be rejected whilst lighter particles are carried to the burners in a controlled fuel/air mixture.

INPUTS

COAL FEED RATE

AIR TEMP.

AIR FLOW RATE

PULVERISED
FUEL MILL

PRIMARY OUPUT

FUEL OUTPUT

PRIMARY AIR
DIFF.
PRESSURE

MILL
DIFF.
PRESSURE

MILL
OUTPUT
TEMP.

MILL
MOTOR
CURRENT

MILL FAN
CURRENT

SECONDARY OUTPUTS
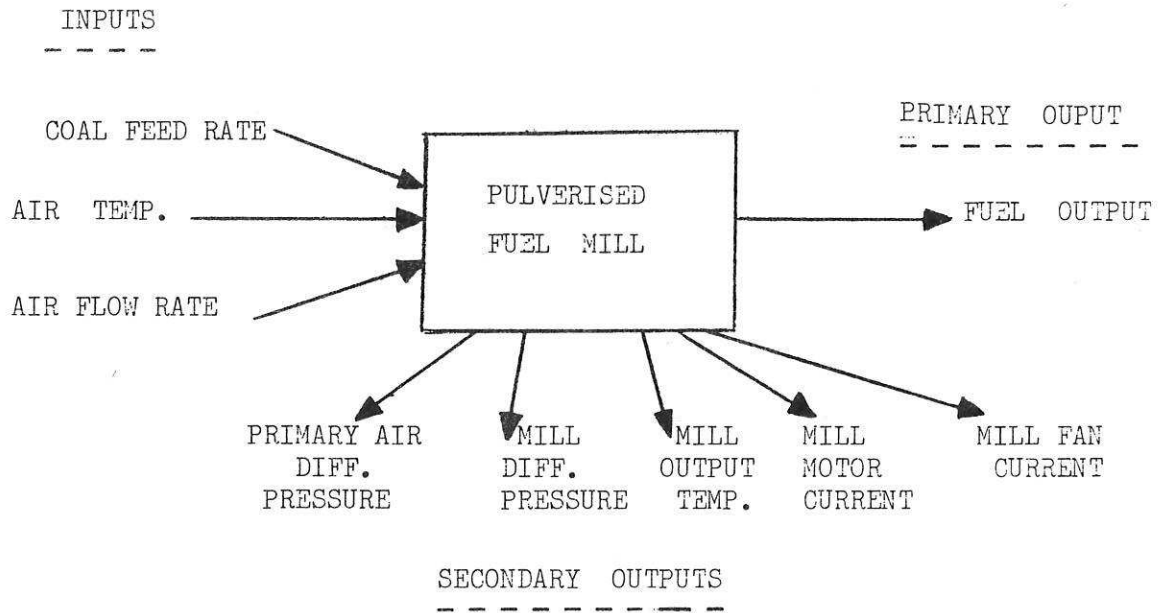
Figure   2.1 a : Pulverised Fuel Mill : Inputs and Outputs

FEED → GRINDING → COARSE CLASS-IFICATION → FINE CLASS-IFICATION → P.F. OUTPUT → FURNACE

DELAY

RECIRCULATION
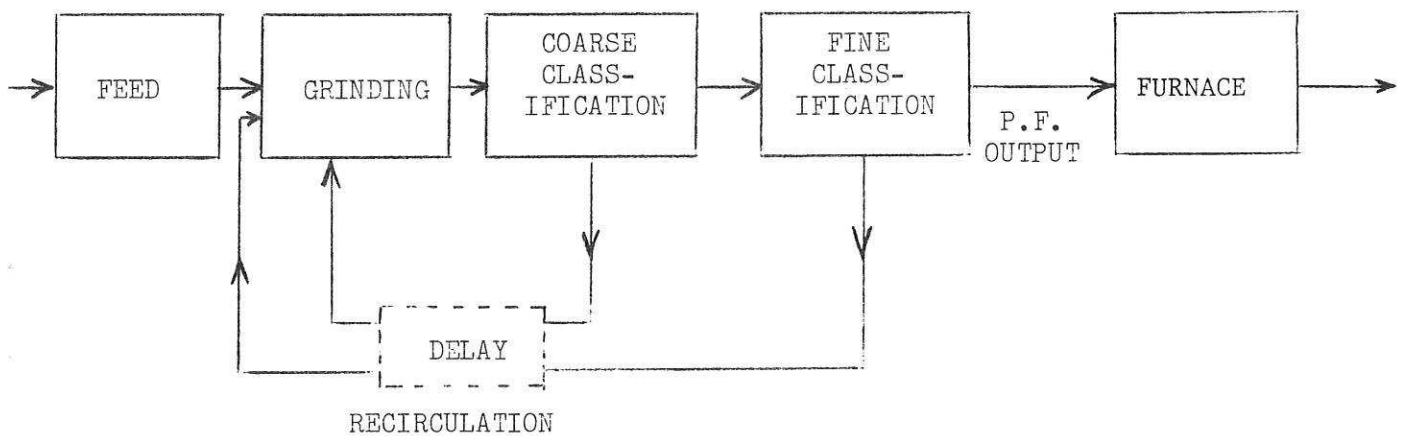
Figure   2.1 b : Pulverised Fuel Mill : Principal Processes

Inputs to the mill are the primary air flow rate, the coal feed rate, and the position of the damper controlling the flow of hot/cold air to the mill. The principal output, the pulverised fuel (p.f.) flow rate, is unobservable on a routine basis but may be inferred from the pressure drop across the primary air fan (PA differential pressure), the pressure drop across the entire mill (mill differential pressure), and the mill outlet temperature. Mill motor current and PA fan current are among other variables available as secondary outputs. The pressure drop in the air passing through the mill has two components: frictional loss due to passage of air through an aperture, and loss due to fuel/air interaction. A square-law relationship may be demonstrated between air flow and frictional loss, whereas the coal-dependent component is directly proportional to the mass of coal in the mill, and largely independent of air flow, see figure 2.3.

Under normal operating conditions it is required to control the boiler master pressure to a particular desired value, determined by grid conditions and consumer demand. A incremental, tuned PID controller operates on the error in master pressure, and the required change in fuel input to the furnace is calculated. This is converted to a demanded fuel change per mill, and then to a common desired primary air differential pressure which is transmitted to all running mills. A separate control program controls the primary air flow for each of the mills, following denormalisation of the desired value to account for individual mill dynamics. The coal feeder speed is controlled to maintain a constant ratio between the primary air differential pressure (ΔP_a) and the mill differential pressure (ΔP_m), termed the 'mill ratio' and represented by the upper line in figure 2.3. The lower line, termed the 'clean air line', is the ratio with no coal in the mill; the difference in ΔP_m between these two lines is thus an indication of the instantaneous fuel in the mill. The mill outlet temperature is separately controlled by adjustment of the dampers supplying hot and cold air to the mill.
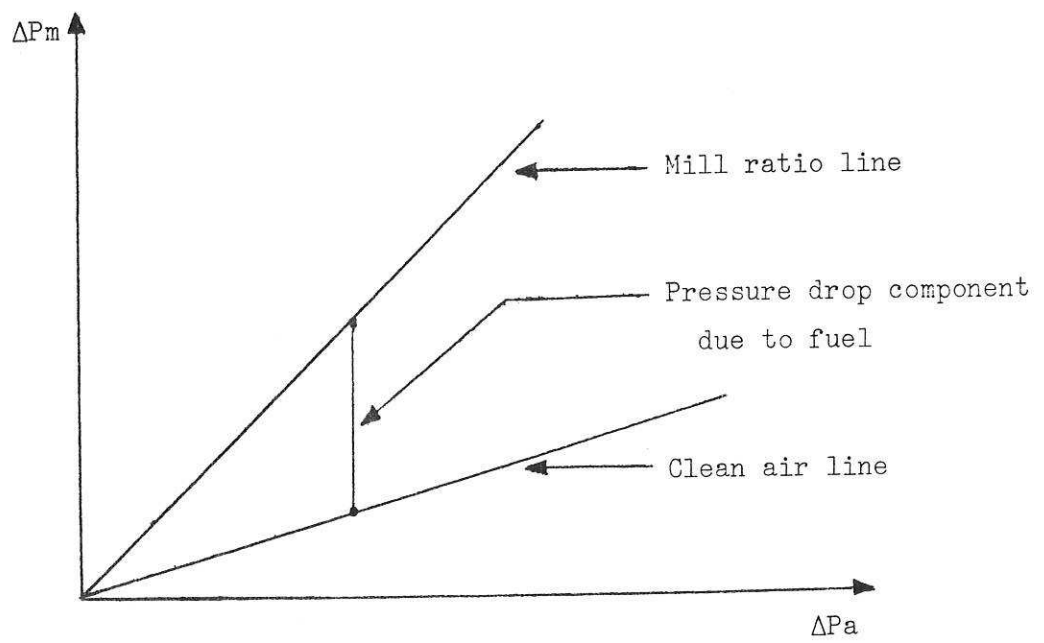
Figure 2.3

As has already been mentioned, pulverised fuel output is not directly observable during routine operation. It is desirable that the mathematical relationship between this quantity and those variables which are routinely available be identified. The exercise reported here is a preliminary step towards such a goal. The fluctuation in boiler master pressure is taken as the variable most closely reflecting changes in pulverised fuel output.

3. Data Collection and Analysis

Data was recorded continuously on magnetic tape during routine operation over a series of twenty-minute periods. A maximum of four channels per test was permitted by the available equipment. The four variables recorded were:

BMP	Boiler master pressure	(output)
ΔP_m	C mill differential pressure	(input 1)
ΔP_a	C mill primary air differential pressure	(input 2)
MFS	C mill feeder speed	(input 3)

These quantities are represented by 1 to 5 volt signals:

BMP	1-5 volts : 0-200 Bar
ΔP_m	1-5 volts : 0-70 mBar
ΔP_a	1-5 volts : 0-7 mBar
MFS	1-5 volts : 0-100%

The recorded data was subsequently sampled at 5 second intervals and stored on disc using the Modular Interface (MINC) computer. This unit was selected for the data-logging operation because of the 12-bit accuracy of the digital-to-analogue converters. The data was thus read to an accuracy of 0.02%. Following this, different data sets were selected: one is used in the identification procedure with the others used for model validity tests. Only two subsets of data showed appreciable variations in plant variables, and these two were transferred to the Perkin-Elmer 3220 for processing using the LMI package.

Figure 3.1 shows the input/output data sequences. The data was first normalised by removal of the mean levels, the normalised data being shown by Figure 3.2.

Correlation analysis between the output and the three inputs was conducted to gain preliminary information regarding the basic plant couplings. Figure 3.3 shows the cross-correlation plots, from which it may be seen that all three inputs are highly correlated with the output. At least one non-zero coefficient is therefore expected for each input in the estimated model. Cross-correlation between the inputs was investigated, and the results are presented in figure 3.4, indicating high correlation between the three selected inputs. Some difficulty must therefore be expected in applying the structural identification method used in the LMI package.

4. Structural and Parametric Identification

The LMI multivariable identification package (Hamiane, 1984) uses a canonically observable form of system representation (Luenberger, 1967) which decomposes the system state equations into n subsystems, where each ith subsystem (i = 1 ... n) is completely observable from the ith output component. This greatly simplifies the problem of multivariable identification, which therefore consists of the estimation of n separate subsystem models associated with each of the n system outputs. Unfortunately, associated with this simplicity is the disadvantage that the use of canonical forms is critically reliant upon correct estimation of the structural indices, and parameter estimates will not be consistent if the structural invariants are wrongly estimated (Ljung, 1976).

State space formulations are the forms of system representation most appropriate to the majority of applications of control systems theory. However, to identify a system model from input-output data sets, a polynomial matrix input-output difference equation representation is more useful. Such an equivalent polynomial matrix representation can be readily derived from the

INPUT 1 (ΔPa)

+5 E 2

47   94   141   188   235

-5

INPUT 2 (ΔPn)

+4 E 2

47   94   141   188   235

-4

INPUT 3 (MFS)

+5 E 2

47   94   141   188   235

-5

OUTPUT (BMP)

+4 E 2

47   94   141   188   235

-4

Figure   3.1

INPUT 1

+3 E 2

2E6

+2 E 2

INPUT 2

2E6

+2

+3 E 2

INPUT 3

2E6

+3

+8 E 1

OUTPUT

2E6

+8
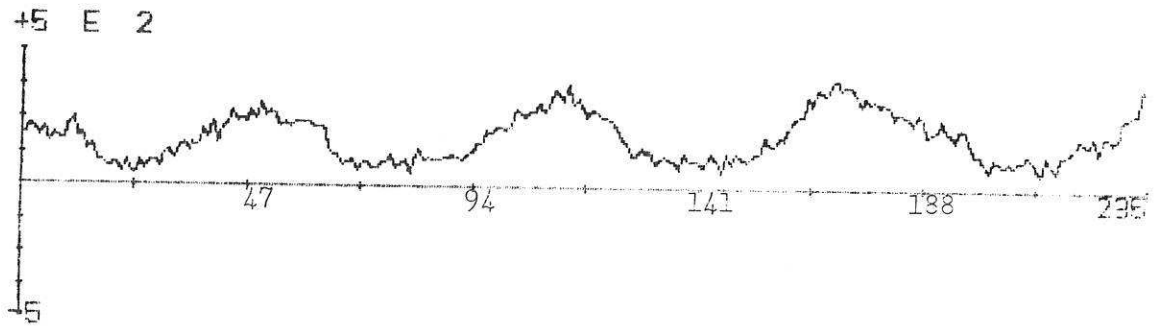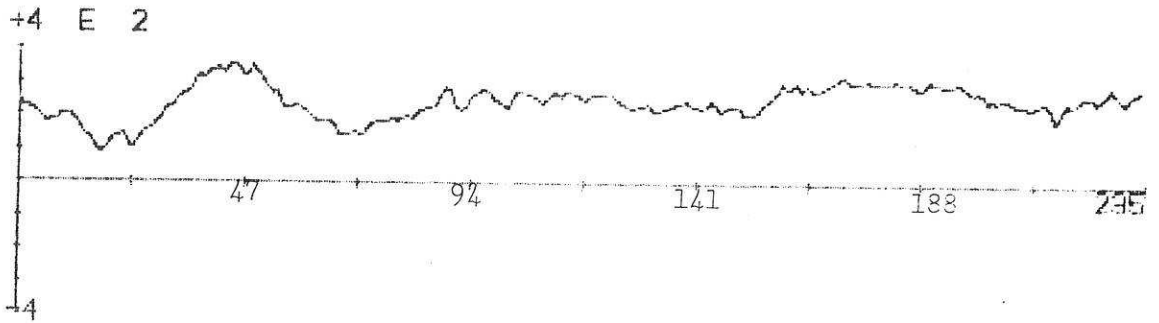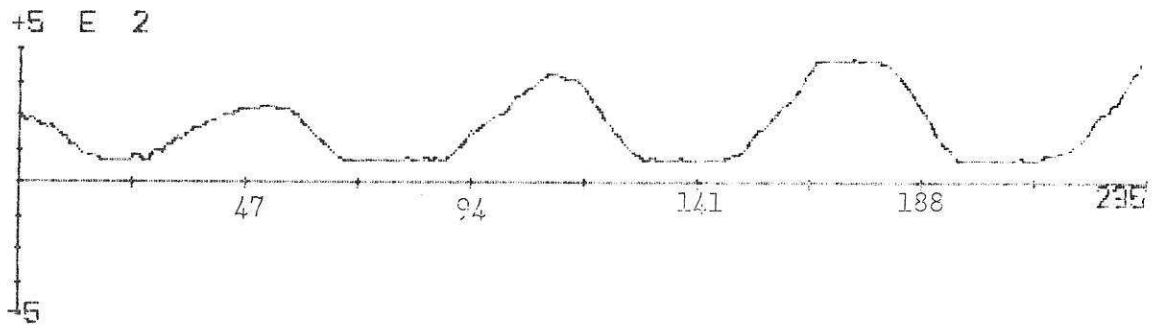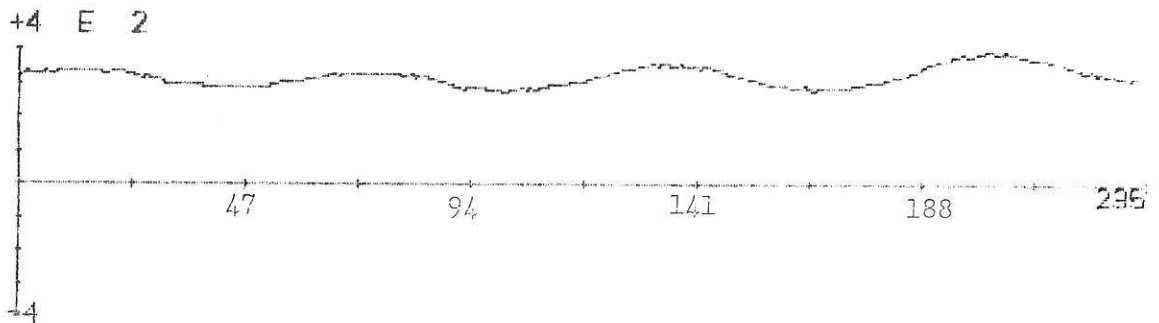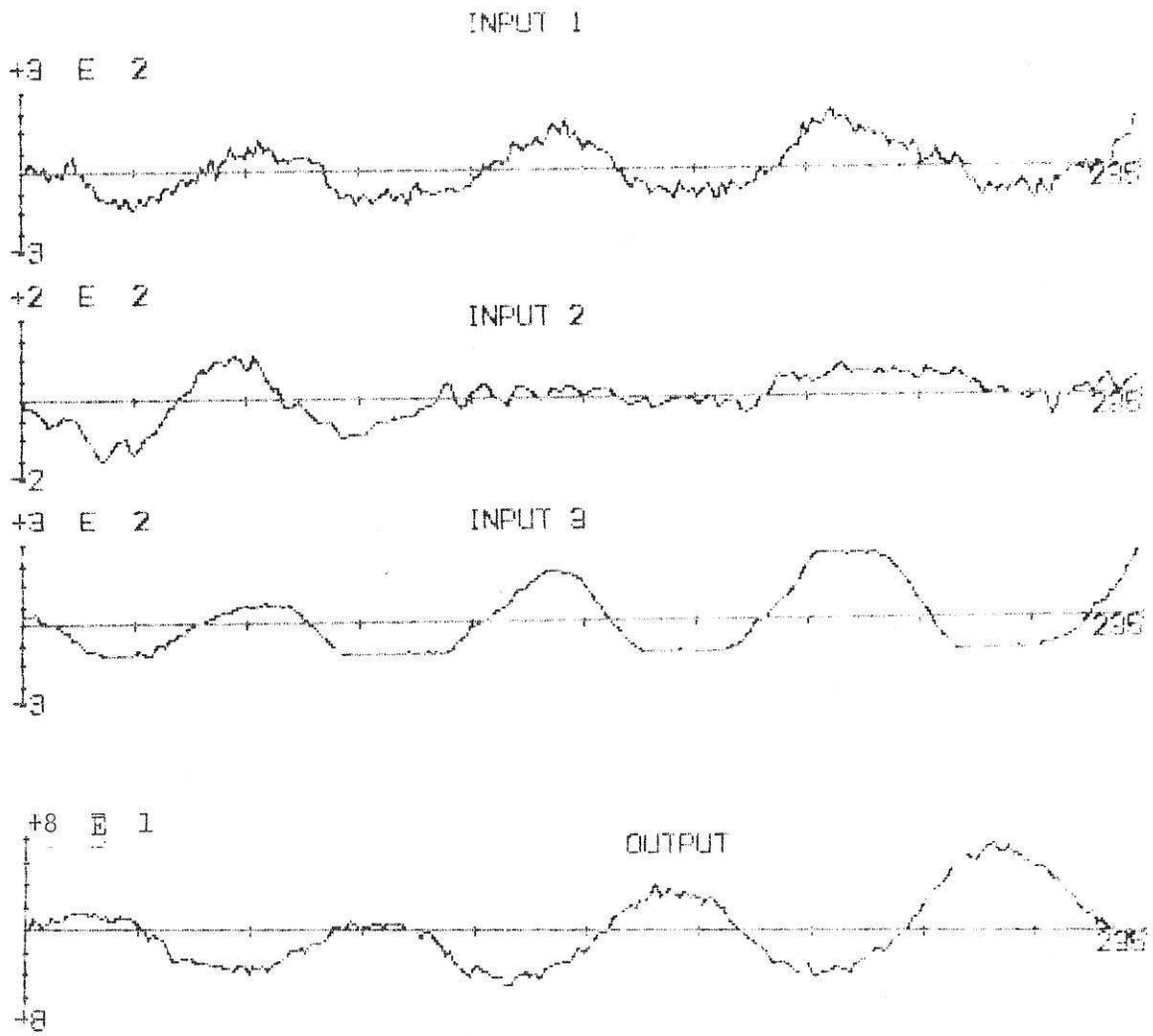
Figure   3.2

CCF BETWEEN INPUT 1 & OUTPUT 1
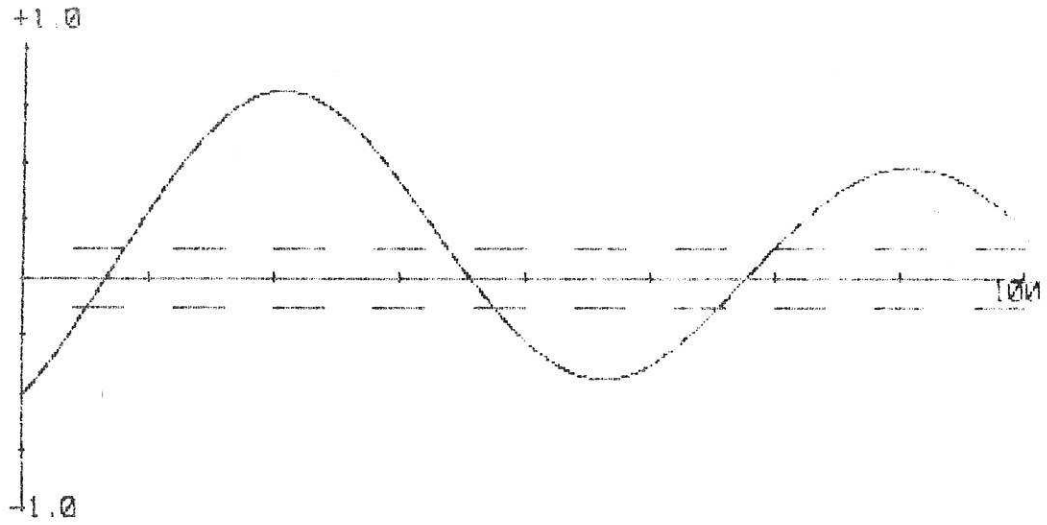
CCF BETWEEN INPUT 2 & OUTPUT 1
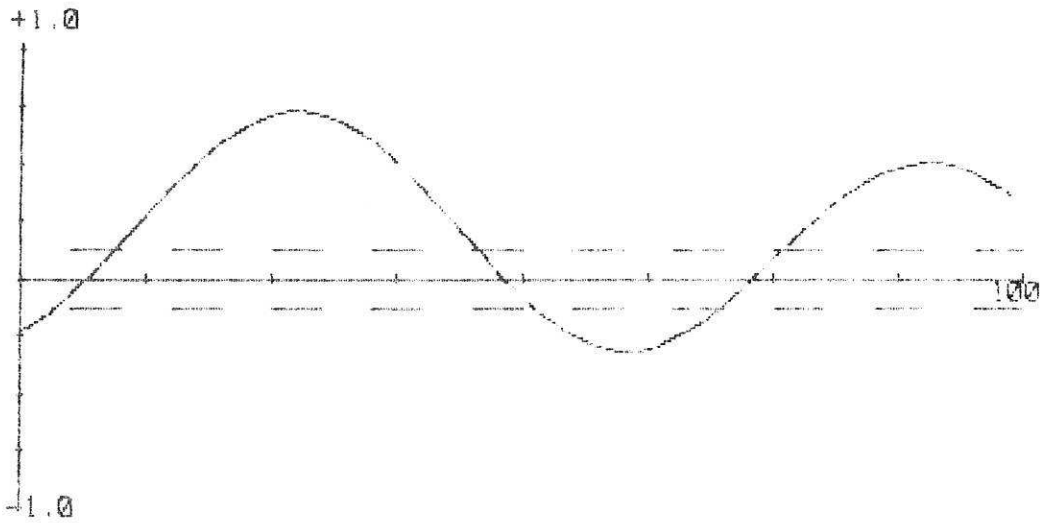
CCF BETWEEN INPUT 3 & OUTPUT 1
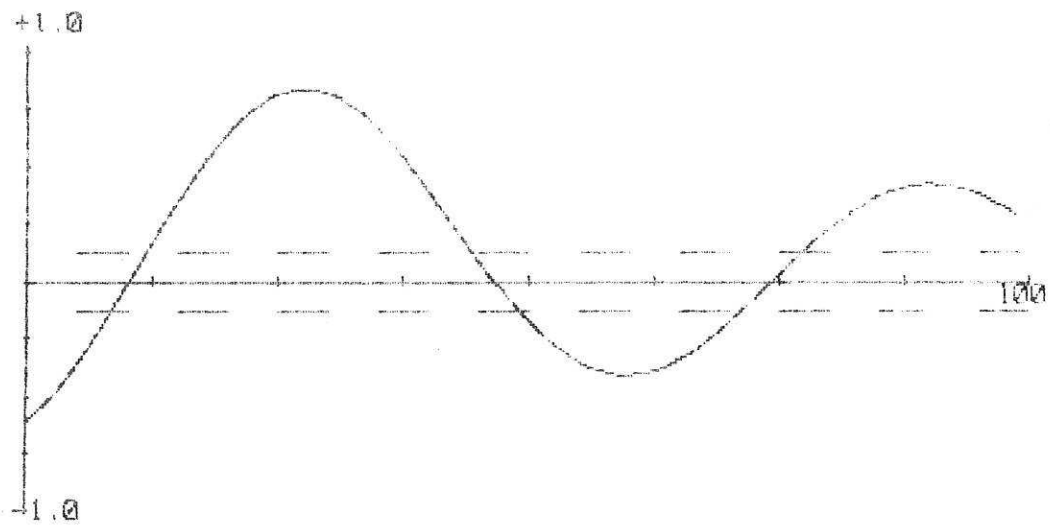
Figure   3.3

CCF BETWEEN INPUT 1 & INPUT 2
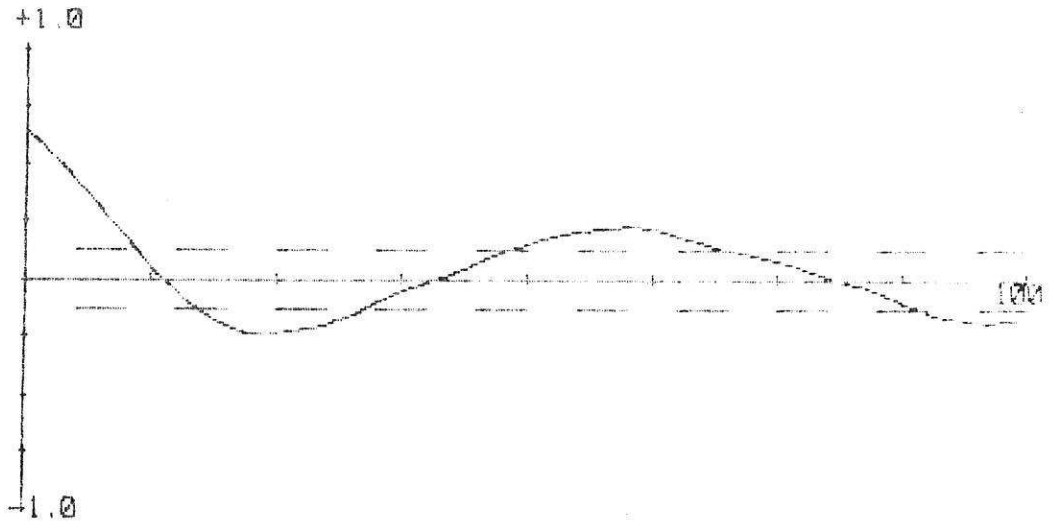
CCF BETWEEN INPUT 1 & INPUT 3
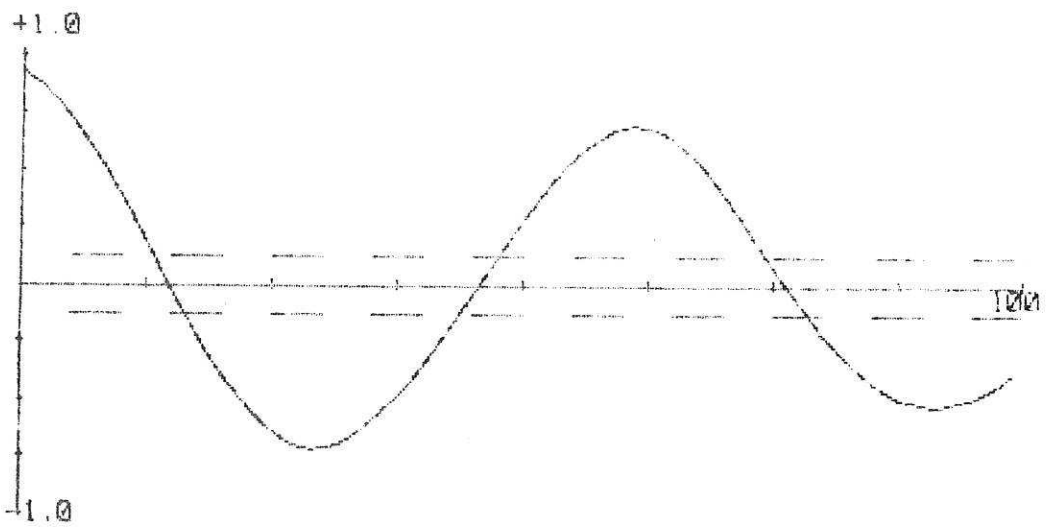
CCF BETWEEN INPUT 2 & INPUT 3
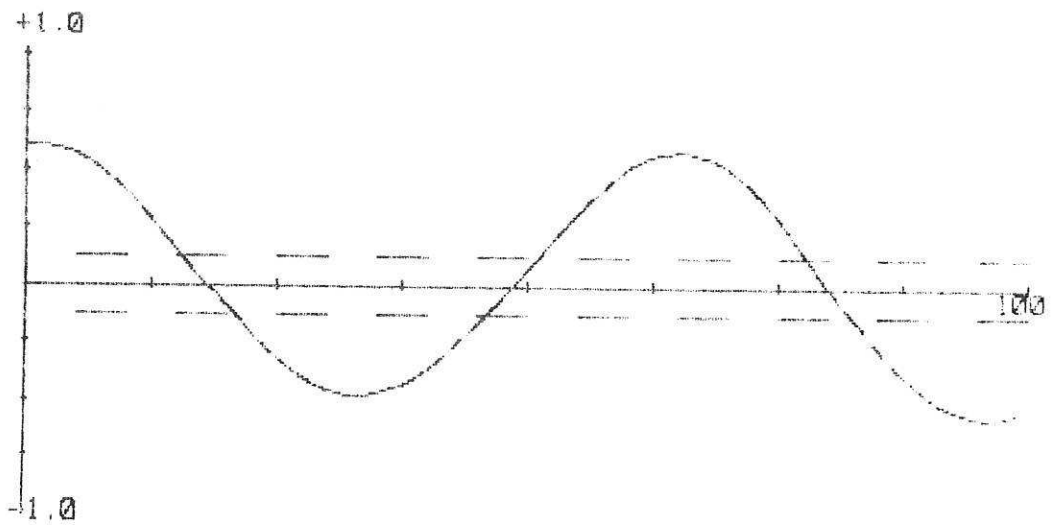
Figure   3.4

canonically observable state-space form (Guidorzi, 1979) and it is this form which is used for identification purposes in the package.

The structural parameters of the observable canonical form are determined using a linear dependence test (Hamiane, 1984). The package then offers four alternative parametric estimation algorithms, conventional recursive least-squares, extended recursive least squares, recursive instrumental variables and recursive suboptimal least squares.

The data from the first data set referred to in section 3 was used to estimate the order, time delays and parameters of the mill model. Subsequent to this, cross-validation was carried out against data from the second data set. Since there is one recorded output, only one subsystem is to be estimated, which is described by the following three-input, one-output model:

$$p(z)Z(k) = q_1(z)u_1(k-d_1) + q_2(z)u_2(k-d_2)$$
$$+ q_3(z)u_3(k-d_3)$$

where $p(z) = a_n + a_{n-1}z + a_{n-2}z^2 + \ldots + z^n$

$$q_1(z) = \beta_{in} + \beta_{i,(n-1)}z + \beta_{i,(n-2)}z^2 + \ldots + \beta_{i1}z^{n-1}$$

n is the model order and d_1, d_2 and d_3 the time delays between the output and inputs u_1, u_2 and u_3 respectively.

4.1 Structure determination

As stated in Section 3 the high correlation between the inputs makes the structure determination method available in the package inadequate for this application. Figure 4.1 indicates a first order model for zero delay to all the inputs. However, by assuming a common delay for all the input/output channels, the conventional iterative method (Hamiane, 1984) (Estimation rule 2) indicated that a fourth order model with a common delay of 6 was a better description of the system. Using the recursive extended least-squares 1, a minimum of the loss function was sought by varying the common time delay

SUBSYSTEM NO. 1

SOS RESIDUAL ERROR TEST
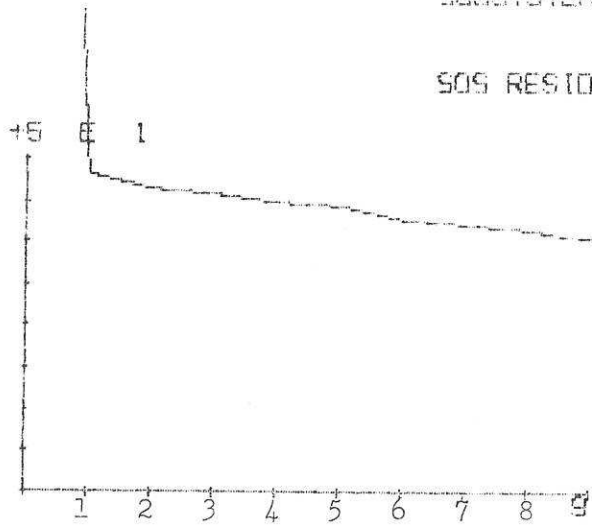
| RESIDUAL ERROR	ORDER
29.1061900E+01	0
47.4099700E+00	1
45.3749900E+00	2
44.4319600E+00	3
43.2757900E+00	4
42.7059500E+00	5
40.6824500E+00	6
39.9337900E+00	7
39.0079700E+00	8
37.7795600E+00	9

Figure   4.1
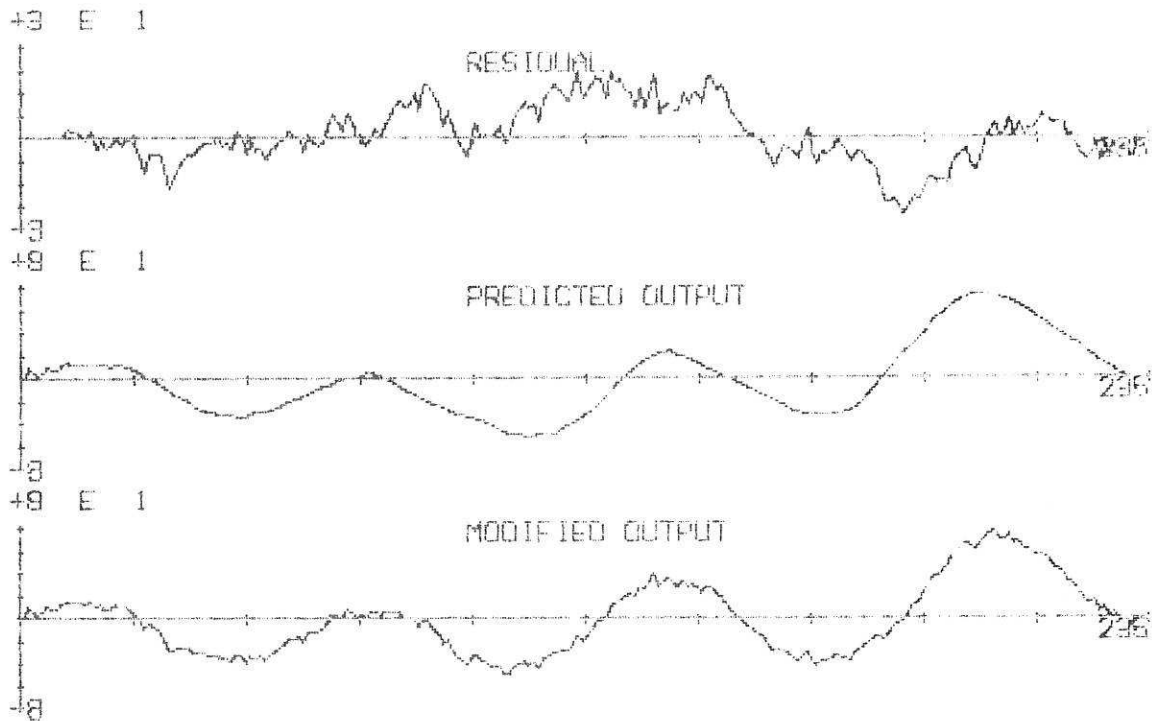
Figure   4.2

whilst maintaining a constant model order. This procedure was repeated for various values of model order and the set $\{n, d_1 = d_2 = d_3\}$ which led to minimisation of the loss function was selected.

This set was also chosen such that a further increase in the model order did not significantly change the value of the loss function. Table 4.1 indicates that

$$n = 4 \text{ and } d_1 = d_2 = d_3 = 6$$

A model order of 4 implies that there are 16 parameters to be estimated in the process model.

4.2 Parameter estimation

Parameter estimation was performed using the recursive least-squares (RLS), the recursive extended and suboptimal least-squares (RELS and RSOLS) and the recursive instrumental variable (RIV) algorithms with the above values for model order and common time delay, and four passes over the data set.

4.2.1 Recursive least-squares (RLS)

The RLS algorithm was applied and yielded the following estimated model consisting of 16 coefficients.

$Z(k) = 0.01536\ Z(k-4) - 0.07574\ Z(k-3) +$

$\qquad + 0.15938\ Z(k-2) + 0.72377\ Z(k-1) +$

$\qquad + 0.01965\ u_1(k-10) + 0.01156\ u_1(k-9) +$

$\qquad - 0.00803\ u_1(k-8) - 0.01526\ u_1(k-7) +$

$\qquad - 0.00413\ u_2(k-10) + 0.00110\ u_2(k-9) +$

$\qquad - 0.00730\ u_2(k-8) + 0.01876\ u_2(k-7) +$

$\qquad + 0.02179\ u_3(k-10) + 0.02902\ u_3(k-9) +$

$\qquad - 0.01581\ u_3(k-8) - 0.01807\ u_3(k-7)$

Figure 4.2 compares the predicted and process outputs, displaying good correspondence. The residuals were analysed using the model validity checks and are shown in figure 4.3, indicating that the estimates are biased.

Order \ Delay	0	1	2	3	4
1	$73.221 \ 10^3$	$36.952 \ 10^3$	$31.916 \ 10^3$	$14.910 \ 10^4$	$37.105 \ 10^3$
2	381.197	249.924	291.977	365.433	428.675
3	177.034	129.425	167.415	159.955	265.103
4	110.545	100.113	123.812	113.416	115.645
5	107.861	98.233	115.681	99.310	99.754
6	103.931	97.560	99.841	97.265	97.948

Order \ Delay	5	6	7	8
1	$34.423 \ 10^3$	$65.101 \ 10^2$	$50.575 \ 10^2$	942.896
2	367.605	260.67	175.213	168.892
3	149.342	124.23	116.785	106.346
4	115.766	97.365	97.671	96.859
5	99.782	96.274	95.196	96.597
6	97.052	94.555	94.234	95.423

TABLE 4.1

Variations of Loss Function with increasing
values of model order and time delay

ACF OF RESIDUALS

CCF BETWEEN RESIDUALS & INPUT 1

CCF BETWEEN RESIDUALS & INPUT 2

CCF BETWEEN RESIDUALS & INPUT 3
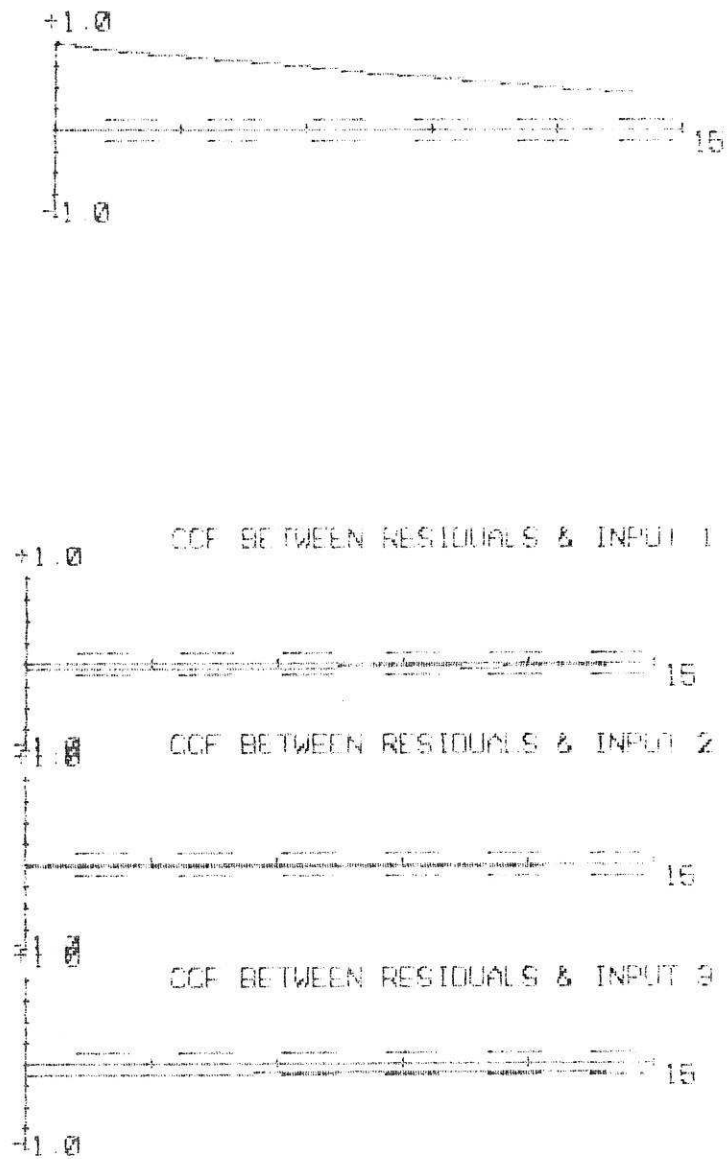
Figure   4.3

Biased estimates are expected (Hamiane, 1984) when the RLS estimator is applied to real processes, as these are generally corrupted by coloured noise. Furthermore, even if the noise were white, the inevitable external perturbations affecting the recorded data will also lead to bias in the estimates.

4.2.2 Recursive instrumental variable (RIV)

The RIV algorithm was applied to the data and yielded the final model consisting of 16 coefficients:

$$
\begin{aligned}
Z(k) \;=\;\; & 0.08358\ Z(k-4) && - 0.06815\ Z(k-3)\ + \\
& +\ 0.3941\ Z(k-2) && +\ 0.5677\ Z(k-1)\ + \\
& +\ 0.02002\ u_1(k-10) && +\ 0.01160\ u_1(k-9)\ + \\
& -\ 0.00562\ u_1(k-8) && -\ 0.01790\ u_1(k-7)\ + \\
& -\ 0.01295\ u_2(k-10) && +\ 0.01647\ u_2(k-9)\ + \\
& -\ 0.02331\ u_2(k-8) && +\ 0.02052\ u_2(k-7)\ + \\
& +\ 0.02773\ u_3(k-10) && +\ 0.02834\ u_3(k-9)\ + \\
& -\ 0.01268\ u_3(k-8) && +\ 0.01969\ u_3(k-7)\ +
\end{aligned}
$$

Inspection of figure 4.4 indicates that the predicted output is comparable with the process output. The estimation errors were processed using the model validity checks and the results are shown in figure 4.5. The correlation coefficients $r_{u_1\xi}(\tau) = 0$, $r_{u_2\xi}(\tau) = 0$ and $r_{u_3\xi}(\tau) = 0$ show that the estimates are unbiased.

4.2.3 Recursive suboptimal least-squares (RSOLS)

The RSOLS algorithm was applied and yielded the final estimated model consisting of 16 coefficients:

$$
\begin{aligned}
Z(k) \;=\;\; & 0.3240\ Z(k-4) && - 0.2186\ Z(k-3)\ + \\
& -\ 0.01982\ Z(k-2) && +\ 0.8779\ Z(k-1)\ + \\
& +\ 0.01204\ u_1(k-10) && +\ 0.01464\ u_1(k-9)\ + \\
& +\ 0.0028\ u_1(k-8) && +\ 0.0095\ u_1(k-7)\ + \\
& -\ 0.01765\ u_2(k-10) && +\ 0.0313\ u_2(k-9)\ +
\end{aligned}
$$
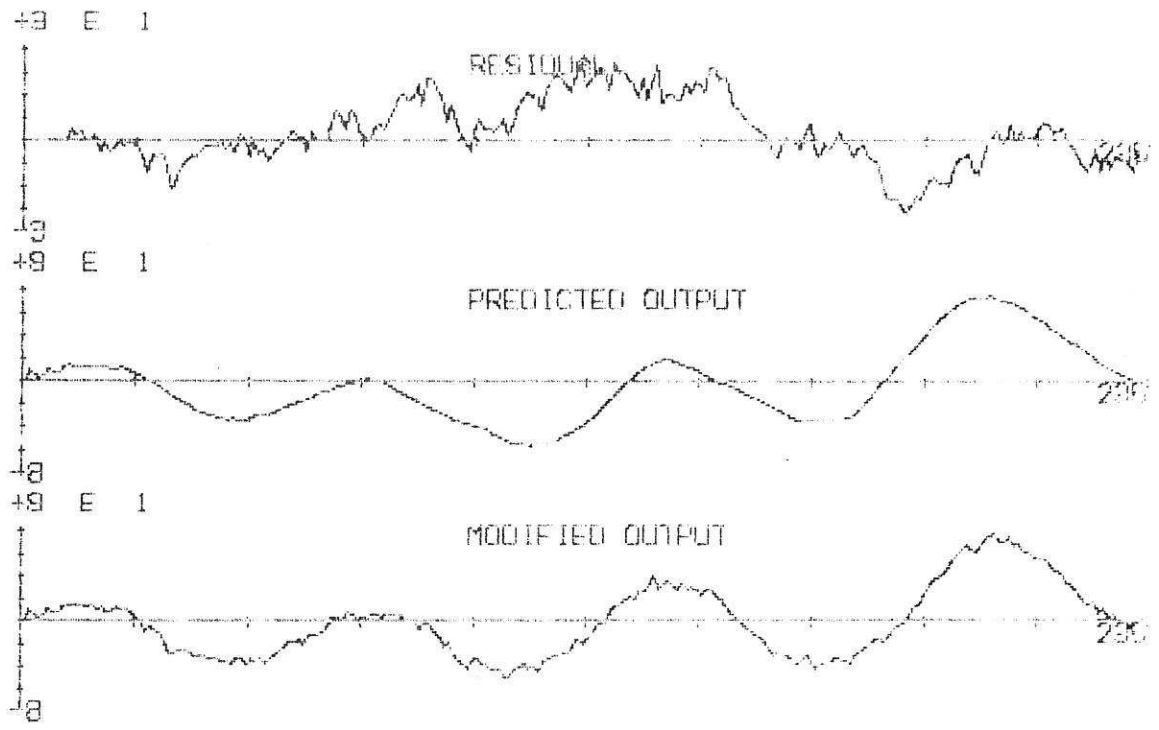
Figure   4.4
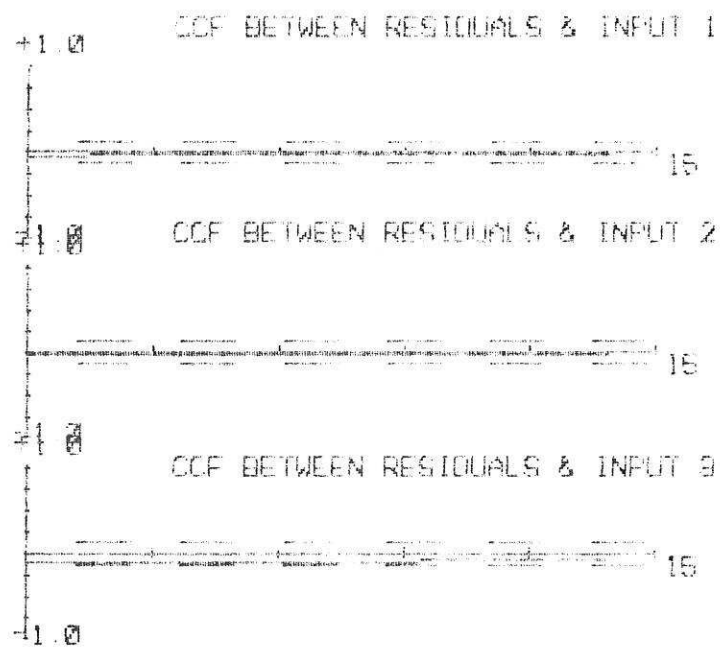
Figure   4.5

$$- 0.05736 \ u_2(k-8) \ + \ 0.0543 \ \ u_2(k-7) \ +$$

$$+ \ 0.01279 \ u_3(k-10) \ + \ 0.00506 \ u_3(k-9) \ +$$

$$+ \ 0.11643 \ u_3(k-8) \ - \ 0.1412 \ \ u_3(k-7)$$

Figure 4.6 shows that the predicted output is comparable with the process output. The estimation errors were processed using the model validity checks and the results are shown in figure 4.7 $r_{u_1\xi}(\tau) = 0$, $r_{u_2\xi}(\tau) = 0$ and $r_{u_3\xi}(\tau) = 0$, indicating that the estimates are unbiased.

4.2.4 Recursive extended least-squares (RELS)

Noise corrupting real processes is generally assumed to be coloured and hence only the first version of the RELS algorithm was applied, i.e. RELS I. It is important to note however, that if the output were known to be corrupted by white noise then, because the model has only one output, the RELS I and RELS II algorithms would yield the same results, provided the noise model order is taken to be equal to the process model order, as was the case here. The RELS I algorithm yielded the following estimated model consisting of 20 coefficients :

$$Z(k) \ = \ 0.06912 \ Z(k-4) \ \ - \ \ 0.06424 \ Z(k-3) \ +$$

$$+ \ 0.3712 \ \ \ Z(k-2) \ + \ 0.5977 \ \ \ Z(k-1) \ +$$

$$+ \ 0.01859 \ u_1(k-10) \ + \ 0.01233 \ u_1(k-9) \ +$$

$$- \ 0.00852 \ u_1(k-8) \ \ - \ 0.01437 \ u_1(k-7) \ +$$

$$- \ 0.00697 \ u_2(k-10) \ + \ 0.003862 \ u_2(k-9) \ +$$

$$- \ 0.007672 \ u_2(k-8) \ + \ 0.01967 \ u_2(k-7) \ +$$

$$+ \ 0.02532 \ u_3(k-10) \ + \ 0.02865 \ u_3(k-9) \ +$$

$$- \ 0.01476 \ u_3(k-8) \ \ - \ 0.02073 \ u_3(k-7) \ +$$

$$- \ 0.02905 \ e(k-4) \ \ \ + \ 0.07603 \ e(k-3) \ +$$

$$- \ 0.1417 \ e(k-2) \ \ \ \ + \ 0.1501 \ e(k-1)$$

Inspection of figure 4.8 indicates that the predicted output compares favourably with the process output. The residual errors were analysed using correlation checks and these are shown in figure 4.9. $r_{\xi\xi}(\tau) = 0$ indicates

RESIDUAL

PREDICTED OUTPUT

MODIFIED OUTPUT

Figure 4.6

CCF BETWEEN RESIDUALS & INPUT 1

CCF BETWEEN RESIDUALS & INPUT 2

CCF BETWEEN RESIDUALS & INPUT 3
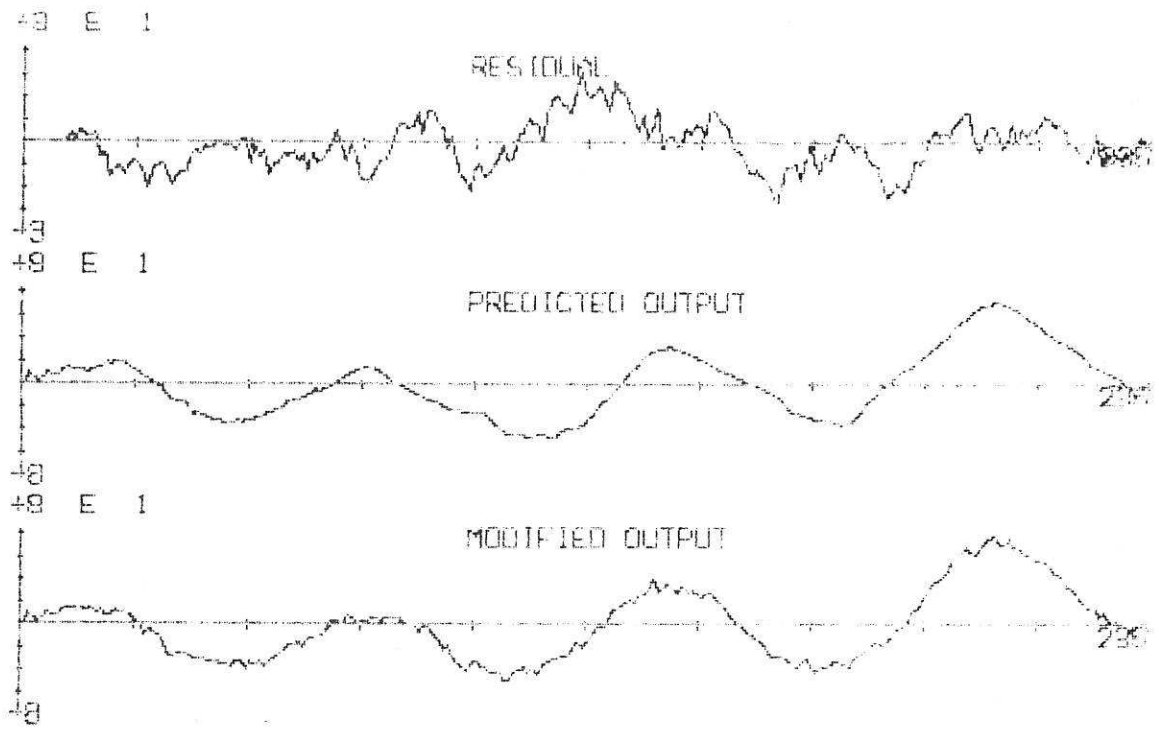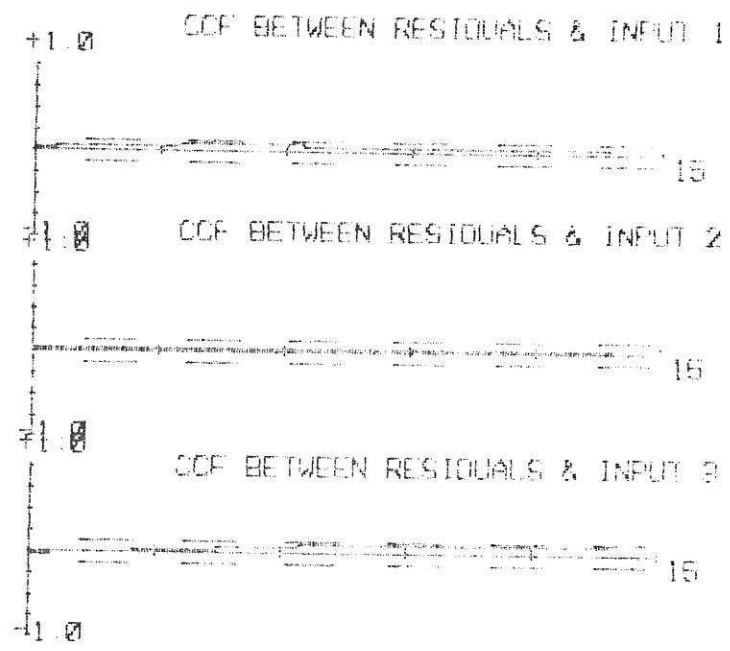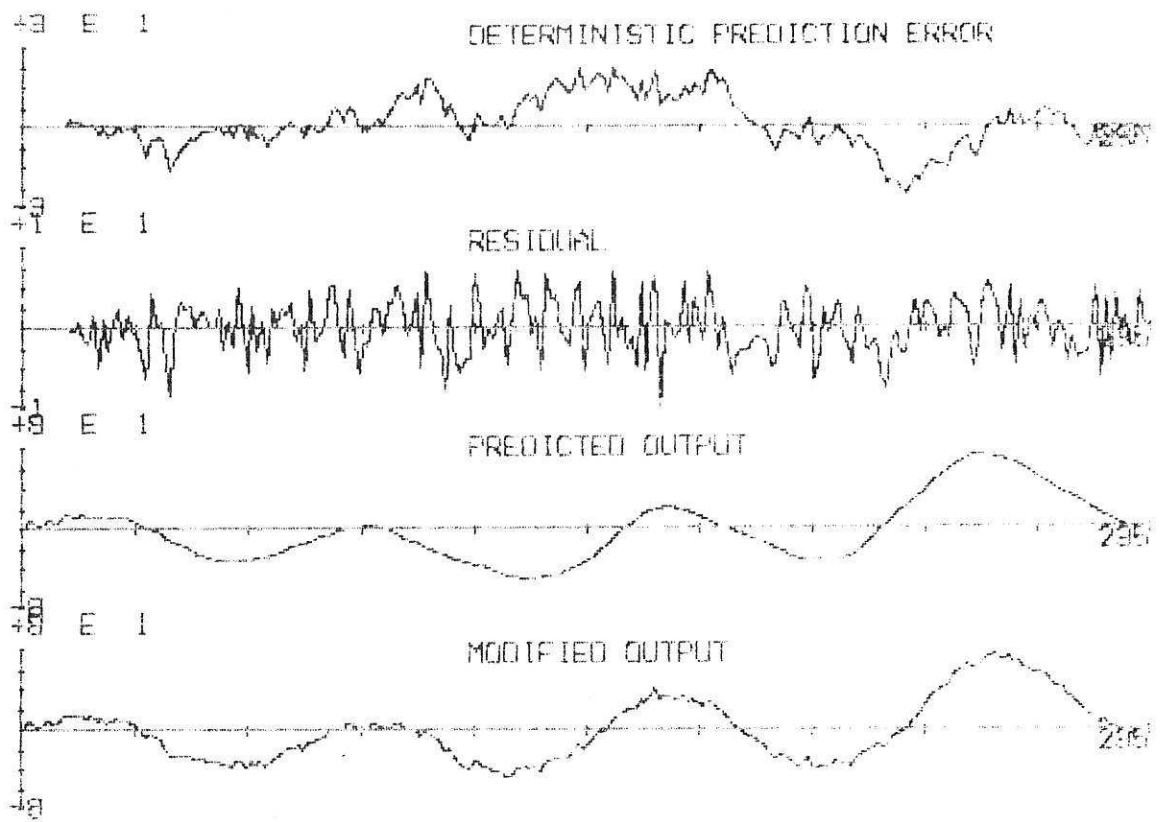
Figure 4.7

Figure   4.8

ACF OF RESIDUALS

CCF BETWEEN RESIDUALS & INPUT 1

CCF BETWEEN RESIDUALS & INPUT 2

CCF BETWEEN RESIDUALS & INPUT 3
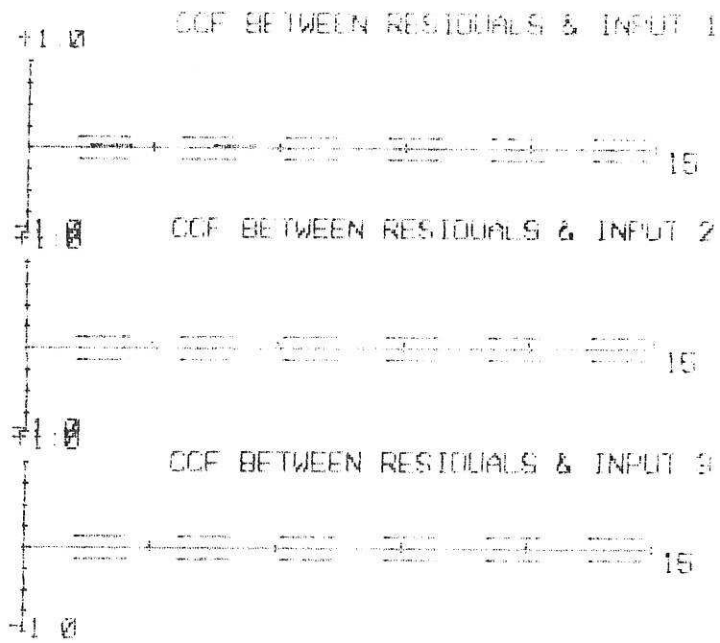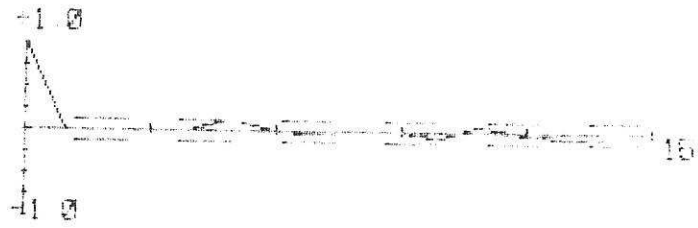
Figure   4.9

that the residuals are white and $r_{u_1\xi}(\tau) = 0$, $r_{u_2\xi}(\tau) = 0$ and $r_{u_3\xi}(\tau) = 0$ indicate that the estimates are unbiased.

Inspection of figure 4.10 showing the predicted outputs of the estimated models obtained by RLS, RIV, RSOLS and RELS I superimposed on the real process output. Inspection of the corresponding model validity tests indicates that the recursive extended least-squares algorithm appears to yield the best model, with the recursive suboptimal least-squares algorithm being the next best, followed by the recursive instrumental variable. The simple least-squares estimator yielded biased estimates, implying that the output noise is coloured, as is the case with most real applications. However, it may be noted from the results given in table 4.2 that the parameter estimates of the RSOLS estimator are not comparable with those of the RLS, RIV and RELS I estimators, which show reasonable agreement. On the other hand, inspection of the predicted output and the model validity tests has indicated that the estimates are unbiased. These contradictory results may be explained as follows: any bias appearing in the coefficients β_{ij} of the input regression may affect the coefficients a_k of the output regression and vice-versa. These two effects may compensate each other in the input-output regression and produce a model output that is comparable with the process output. The bias appearing in the coefficients may be due to the fact that the noise is probably not additive at the output, which results in biased estimates.

The predictivity of the estimated model was then tested by fitting the model to the second set of data. The raw input/output data was first normalised as shown in figure 4.11. The predicted output was then computed using the measured inputs and compared with the real output from the same data set. Figure 4.12 indicates that the predicted output is not comparable with the process output. This implies that the estimated model is not predictive and hence not valid for the process. This may be attributed to operating point dependent non-linearities in the system and to changes in variables beyond
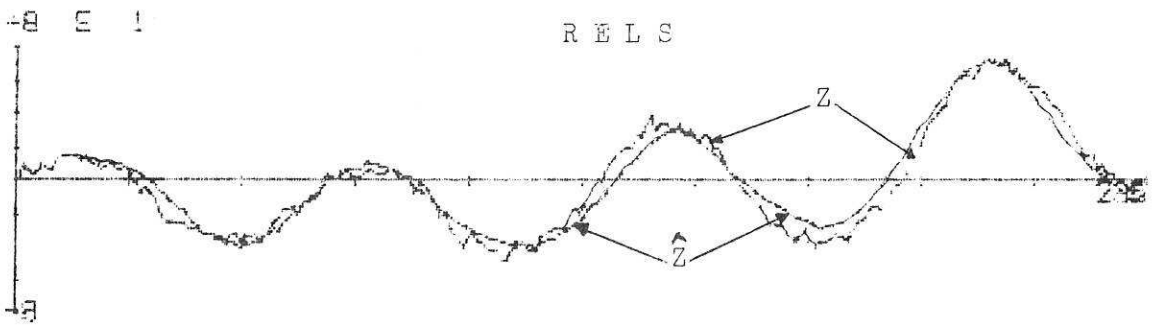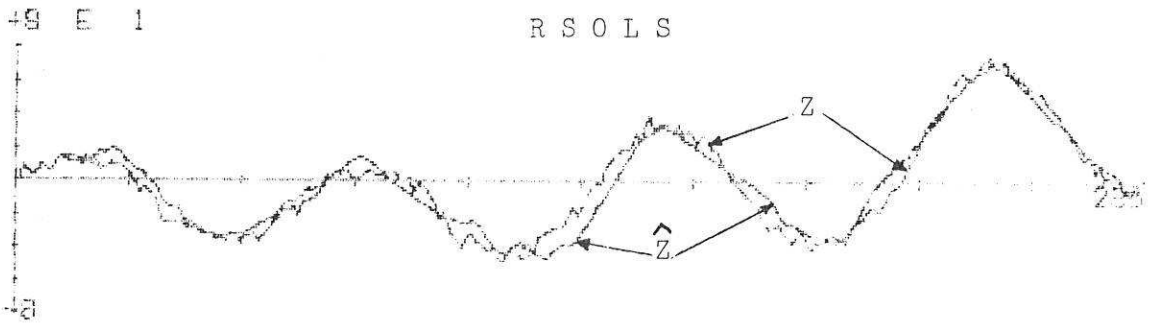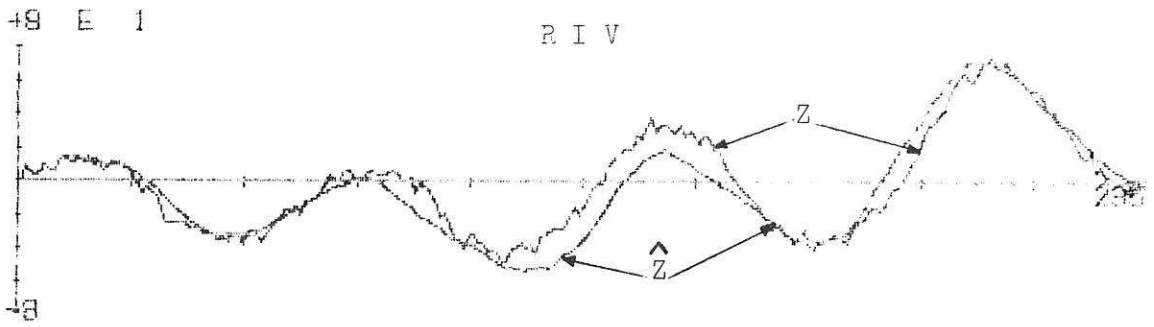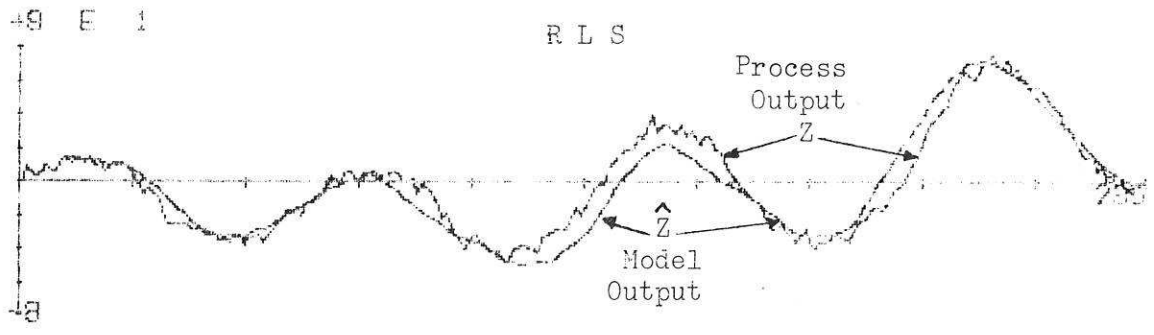
z Process output

ẑ Predicted "

Figure 4.10

| Coefficient	RLS	RIV	RSOLS	RELS I
a_1	0.01536	0.08358	0.3240	0.06912
a_2	-0.07574	-0.06815	-0.2186	-0.06424
a_3	0.15938	0.3941	-0.01982	0.3712
a_4	0.72377	0.5677	0.8779	0.5977
β_{11}	0.01965	0.02002	0.01204	0.01859
β_{12}	0.01156	0.01160	0.01464	0.01233
β_{13}	-0.00803	-0.00562	0.0028	-0.00852
β_{14}	-0.01526	-0.01790	0.0095	-0.01437
β_{21}	-0.00413	-0.01295	-0.01765	-0.00697
β_{22}	0.00110	0.01647	0.0313	0.00386
β_{23}	-0.00730	-0.02331	-0.05736	-0.00767
β_{24}	0.01876	0.02052	0.0543	0.01967
β_{31}	0.02179	0.02773	0.01279	0.02532
β_{32}	0.02902	0.02834	0.00506	0.02865
β_{33}	-0.01581	-0.01268	0.11643	-0.01476
β_{34}	-0.01807	-0.01969	0.14121	-0.02073
c_1				-0.02905
c_2				0.07603
c_3				-0.1417
c_4				0.1501

TABLE   4.2

Comparison between parameter estimates of
RLS, RIV, RSOLS and RELS I algorithms

INPUT 1
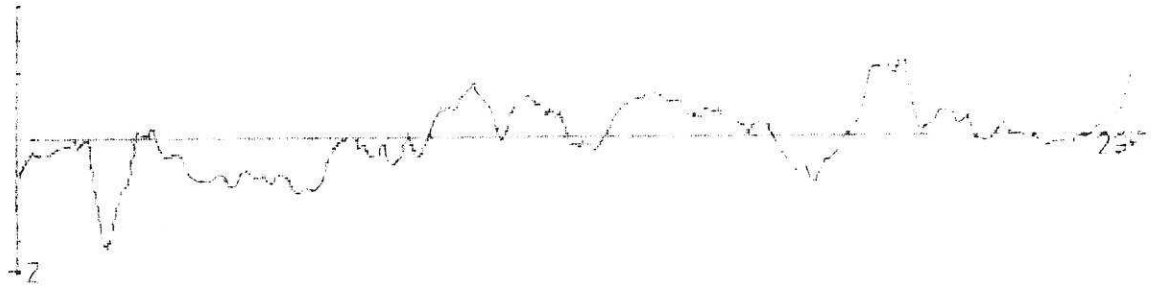
INPUT 2

INPUT 3
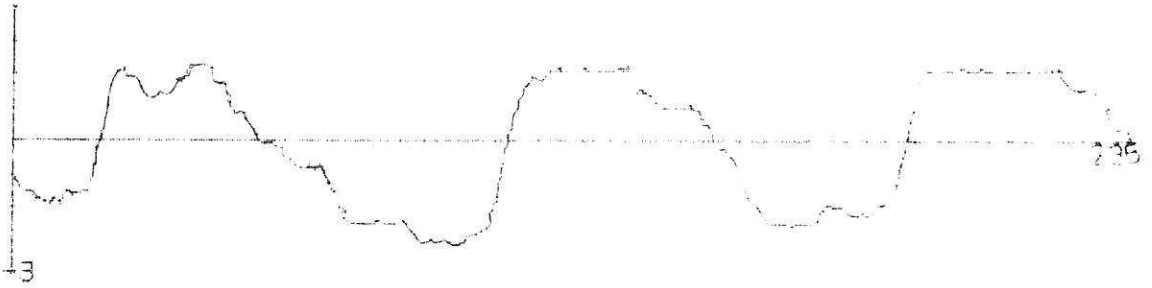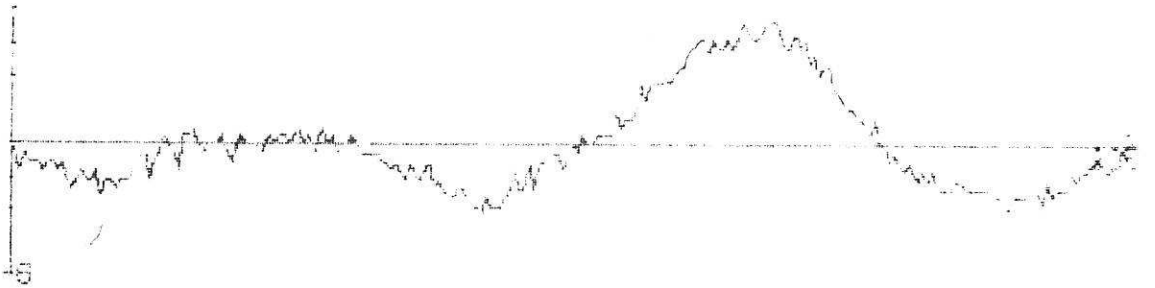
OUTPUT
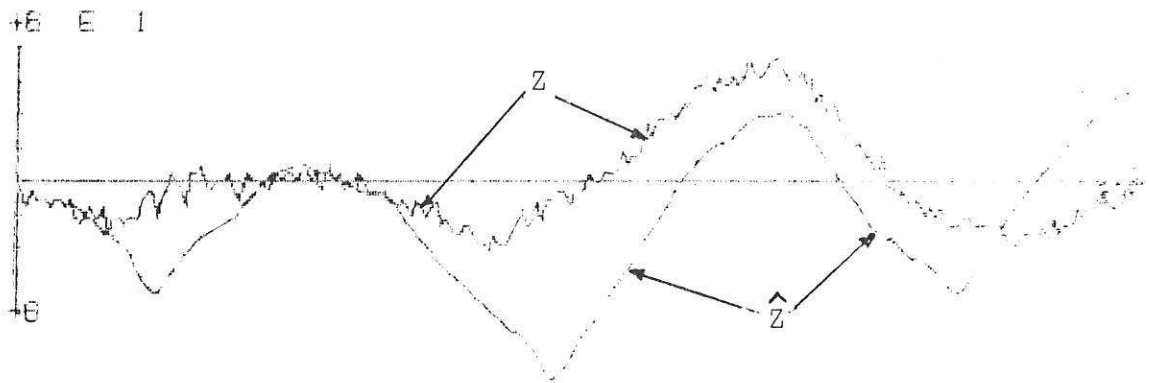
Figure 4.11

Figure 4.12

the measuring capacity of this experiment; for instance, the available data was probably sampled too infrequently, resulting in a substantial loss of information. These poor results may also be attributed to the fact that only four variables were considered in the estimation and hence any existing couplings between the available data and other operating variables have been neglected. It would have been desirable to repeat these tests with other data sets. Unfortunately, within the data recorded only two subsets of data showed appreciable variations in plant variables and no other subsets could be derived.

5. Conclusions

Structural and parametric identification of a pulverised fuel mill is illustrated using the iterative search method for model order and time delay determination and four recursive estimation algorithms for parametric identification. The description of the process and its operation were briefly reviewed. The process was assumed to be linear and data was normalised by subtracting mean levels. Correlation analysis was performed as a preliminary step in the identification procedure in order to verify relations between the different variables. The correlation plots have shown that a high correlation exists between inputs and outputs but also between the inputs, which did now allow fast determination of the structure. A fourth order model with a common delay of 6 to all the inputs was estimated using the recursive least-squares, the recursive suboptimal and extended least-squares and the recursive instrumental variable algorithms. The RELS I algorithm produced the best results with an estimated model consisting of 20 coefficients. Model validity tests using correlation checks have shown that the parameter estimates are unbiased. However, the model obtained does not provide the correct representation of the system, as indicated by cross-validation tests with another data set. It is therefore concluded that either the available data was sampled too slowly leading to a loss of information or that four variables cannot accurately reflect plant operation, and that more

variables should be included in the identification procedure in order to get a more appropriate model. Furthermore, use of persistently exciting inputs is a necessary requirement in system identification, and normal operating inputs do not generally satisfy the condition of persistent excitation. Therefore another possible reason for the above results is that the recorded input signals were not sufficient to excite all the system modes. A more appropriate model would have probably been identified if additional excitations were added to the actual process inputs. The results presented here may be interpreted as illustrative of the procedure that would be followed if data from a more comprehensive and precisely controlled experiment were available.

6. References.

GUIDORZI, R. P. 'Complete sets of invariants and canonical input-output forms for multivariable systems structural and parametric identification' 5th IFAC Symp., Ident. and Sys. Par. Est, Darmstadt, Vol 2, 1979, pp 429-436.

HAMIANE, M. 'Development and Implementation of an identification package for linear multivariable systems' Ph.D. Thesis, University of Sheffield, 1984.

LJUNG, L. and RISSANEN, J. 'On canonical forms, parameter identifiability and the concept of complexity', Proc. 4th IFAC Symp., Ident. and Sys. Par. Est., TBILISI, 1976.

LUENBERGER, D.G. 'Canonical forms for linear multivariable system'. IEEE Trans on Automatic Control, June 1967, pp 290-293.